

# Effects of Young's modulus of epoxy resin on axial compressive strength of carbon fibre

M. MIWA\*, A. TAKENO, Y. MORI, T. YOKOI, A. WATANABE  
*Faculty of Engineering, Gifu University, Yanagido 1-1, Gifu, Japan 501-11*  
*E-mail: miwa@apchem.gifu-u.ac.jp*

Using epoxy resins with various molecular weight between cross-linkings, attempts have been made to estimate the fibre axial compressive strength of pitch-based graphitized fibre, and the effect of Young's modulus of epoxy resins on compressive strength was investigated. The estimated compressive strength of fibre decreases with increasing temperature. This decrease in compressive strength may be accounted for by a decrease in the radial compressing force due to a decrease in the residual thermal stress. There is a linear relationship between the estimated compressive strength and radial compressive force in a temperature range from room temperature to 80 °C. The estimated compressive strength of the fibre increases with increasing Young's modulus of epoxy resins. In order to realize reinforcing fibres with a higher compressive strength, it will be necessary to use a resin matrix with a higher modulus. © 1998 Kluwer Academic Publishers

## 1. Introduction

A method has been reported for measuring the compressive strength of fibres, i.e. if a sufficiently long fibre is embedded in the neighbourhood of the surface of a rectangular beam and the system is subjected to a tensile (or compressive) strain rather than a fibre ultimate strain, according to the bending method, the fibre eventually breaks into many pieces. By measuring the lengths of the broken pieces, the axial compressive strength of the fibre can be estimated in both cases where the tensile strength of fibres is assumed to be uniform [1, 2] and where it is assumed to be variable [3, 4].

Using the latter method, we estimated the compressive strengths of carbon and aramid fibres. It was found that the estimated compressive strength of PAN-based carbon fibres was higher than pitch-based fibres, and that of carbonized fibres (higher strength type) was higher than graphitized fibres (higher modulus type) [1, 2, 4, 5]. Moreover, the axial fibre compressive strength was approximately 10–60% of the tensile strength [4]. It increased with increasing degree of orientation or face spacing of the crystal and increased with decreasing crystal size [5]. In addition, it increased with decreasing fibre diameter [6]. Furthermore, it was increased by surface and/or sizing treatment [7].

As indicated elsewhere [1–7], the compressive strengths of carbon fibres have been effected by the thermal stress generated mainly by both the difference of thermal expansion and Young's modulus of fibre and resin matrix.

In this work, using epoxy resins with various molecular weights between cross-linkings, the effect of Young's modulus of the epoxy resins on the axial compressive strength using our method as described in a previous paper [4], was investigated.

## 2. Experimental procedure

The fibre used in this study was a pitch-based graphitized fibre (high-modulus type, development sample of Tonen). Mechanical properties are shown in Table I. Two kinds of epoxy resins (bisphenol "A" type, Epikote 828 and 834, Yuka Shell Epoxy) and an amine curing agent (S-Cure 661, Kayaku Akuzo) were used to prepare the specimens. These resins and curing agent were mixed to prepare epoxy matrices with various Young's modulus as shown in Table II.

First, tensile test specimens were prepared using 5, 10, 15, 20, 25, 30, and 100 mm gauge lengths to obtain distribution curves of tensile strength for the fibre. The instrument used was a Tensilon UTM-I-2500 type (Orientec), tensile strain rate  $0.1 \text{ mm mm}^{-1} \text{ min}^{-1}$ , and the number of fibres tested was 100 pieces for each gauge length. The results obtained from the fibre tensile strength distribution tests were used to determine Weibull parameters.

Second, test specimens were prepared for measuring storage modulus. The dimension of a test specimen measured 1.5 mm thickness, 6 mm width, and 60 mm length. The test specimens were subjected to tensile tests at increasing rate with temperature of  $3 \text{ }^\circ\text{C min}^{-1}$ , a frequency of 10 Hz, and a distance of grip of 45 mm

\* Author to whom all correspondence should be addressed.

TABLE I Mechanical properties of fibre (at 20 °C); test length 25 mm

Diameter (μm)	10.0
Tensile strength (GPa)	3.53
Young's modulus (GPa)	516
Breaking strain (%)	0.67

to storage moduli with the aid of a dynamic mechanical tester (DDV-25FP, Orientec).

Third, rectangular specimens were prepared for measuring fragment length. Epoxy resin and curing agent were weighed with a weight ratio as shown in Table II. The mixture was agitated thoroughly and then defoamed in a vacuum at 80 °C for 1 h. This mixture was poured into a mould holding a fibre at a constant tension in the neighbourhood of the surface of a rectangular specimen and subjected to curing at 80 °C for 17 h. The specimen was then allowed to cool to room temperature.

The fragment lengths of specimens prepared in this manner were measured i.e. each specimen was subjected to a tensile (or compressive) strain of 4% at a drop rate of the upper heads of 10 mm min<sup>-1</sup> using the four-point bending method under the same conditions as reported previously [1–7]. In this experiment, to investigate the effect of a radially compressive force on the fibre axial compressive strength, measurements were made at 40–100 °C. Over 200 fragments were examined for each experimental condition.

### 3. Results and discussion

The typical strength distributions of graphitized fibre used in this experiment are shown in Fig. 1.

The tensile strength of brittle fibres such as carbon fibres is generally affected by partial flaws. In general, the tensile strength of such fibres is represented by a chain model. This model represents a fibre with a chain consisting of  $n$  pieces of equal links. Applying the weibull distribution function, the probability  $g(\sigma)$  in which a chain of  $n$  links will break at stress  $\sigma$  can be expressed as [8, 9]

$$g(\sigma) = n m \sigma_0^{-1} \left( \frac{\sigma - \sigma_p}{\sigma_0} \right)^{m-1} \exp \left[ -n \left( \frac{\sigma - \sigma_p}{\sigma_0} \right)^m \right] \quad (1)$$

where  $m$ ,  $\sigma_0$  and  $\sigma_p$  are the Weibull parameters. Also, the mean tensile strength,  $(\bar{\sigma}_{t,l})_t$  of the fibre at length  $L$  is given as [8, 9]

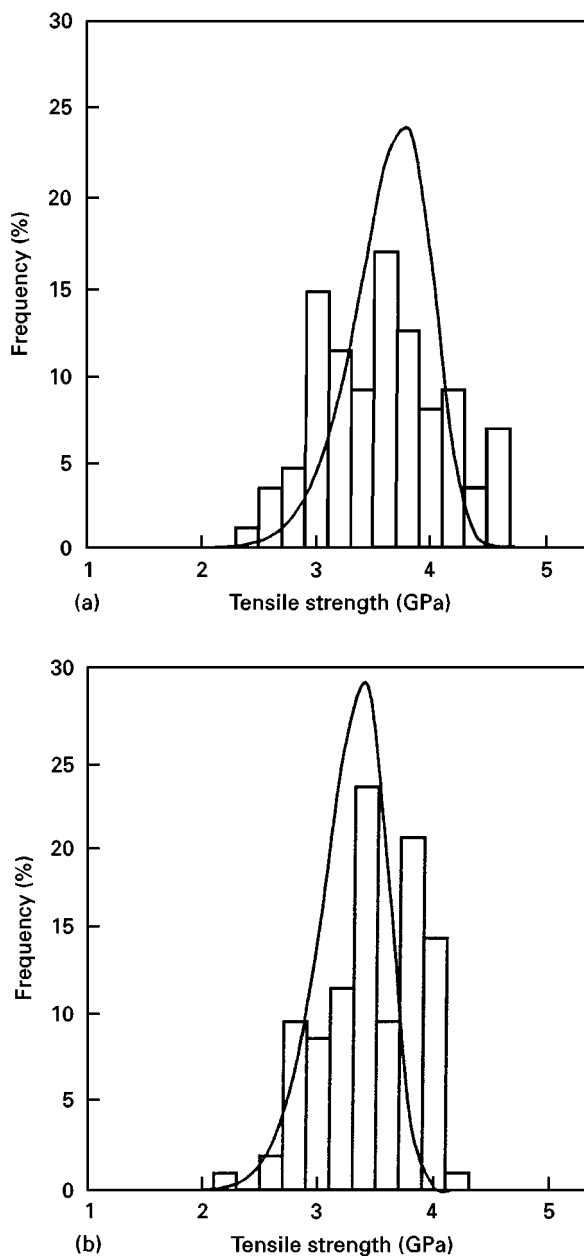


Figure 1 Strength distribution of fibre. (a) Gauge length 25 mm. (b) gauge length 100 mm. (—) Value calculated using Equation 1.

$$(\bar{\sigma}_{t,l})_t = \sigma_p + \left( \frac{\sigma_0}{(L/l_i)^{1/m}} \right) \Gamma \left( \frac{m+1}{m} \right) \quad (2)$$

where  $\Gamma$  is the complete gamma function,  $l_i$  is the length of the link (gauge length  $L$ /number of links  $n$ ) consisting of the fibres.

TABLE II Formulation and properties of epoxy resins

Epikote	Symbol	Resin (p.h.r.)	Curing agent (p.h.r.)	Density (g cm <sup>-3</sup> )	Molecular weight between cross-links
828	828-I	100	2.0	1.175	479
	828-II	100	5.0	1.170	374
	828-III	100	10.0	1.157	366
834	834-I	100	4.0	1.166	443
	834-II	100	8.1	1.160	429

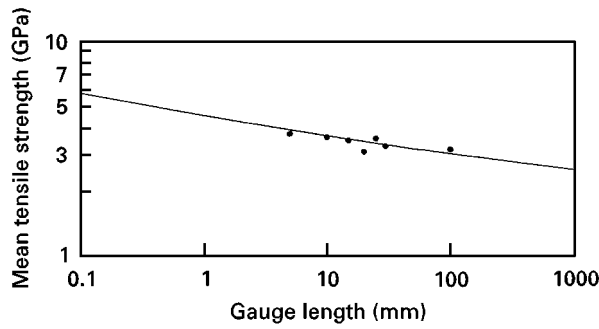


Figure 2 Relation between gauge length and tensile strength. (—) Value calculated using Equation 2.

TABLE III Statistical values of tensile strength for fibre

Weibull parameter		length of links, $l_i$ (mm)
$m$	$\sigma_0$ (GPa)	
7.8	4.85	0.10

The solid line in Fig. 1 represents theoretical values obtained by substituting Weibull parameters  $m$ ,  $\sigma_0$  and  $\sigma_p$  and the length  $l_i$  of links given in Table II into Equation 1.

The relationship between the logarithm of gauge length and the logarithm of the mean tensile strength is also shown in Fig. 2. The solid line in Fig. 2 represents theoretical values calculated by substituting Weibull parameters and the length of the links into Equation 2. The theoretical values obtained by Equations 1 and 2, employing the values of Weibull parameters and the length of the links given in Table III, agree with the measured values. Therefore, the values of Weibull parameters and the length of the links thus determined are valid.

Storage modulus values of epoxy resins are shown in Fig. 3. The storage moduli of 2–3 GPa were obtained at room temperature and 0.01–2 GPa in the region of 80–100 °C.

Nielsen [10] has proposed the following empirical equation which agrees with the experimental results at a various degrees of cross-linking

$$\log_{10} G = 7.0 + 293\rho/M_c \quad (3)$$

where  $G$  is the shear modulus of the specimen,  $\rho$  is the density of the specimen, and  $M_c$  is the molecular weight between cross-linkings.

For isotropic materials the equation,  $E = 2G(1 + \nu)$  is confirmed, where  $E$  is Young's modulus,  $G$  is shear modulus, and  $\nu$  is Poisson's ratio. We assumed  $\nu = 0.49$  in the region of the rubber state and calculated  $M_c$ . The results are shown in Table II.  $M_c$  increases with decreasing content of curing agent. This means that the degrees of cross-linking decrease with decreasing content of curing agent. When the contents of curing agent are 10.0 (Epikote 828) and 8.1 p.h.r. (Epikote 834) for 100 p.h.r. epoxy resin, an absorption ( $914 \text{ cm}^{-1}$ ) in the infrared spectrum by epoxy rings has never been observed. Consequently, it is conceivable that the degree of reaction is about 100%.

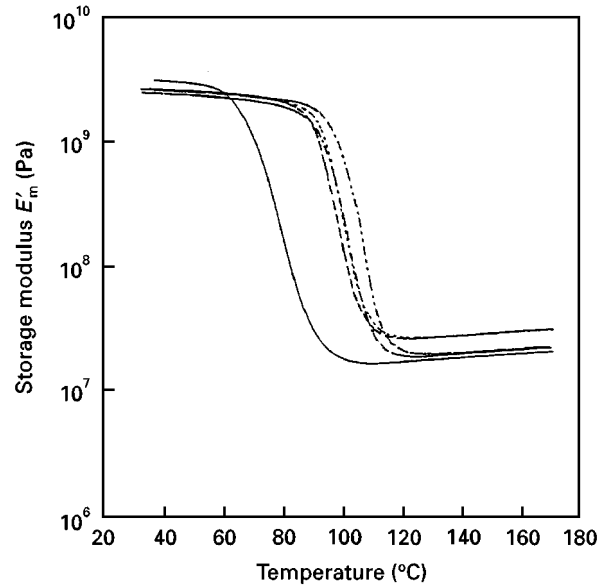


Figure 3 Storage modulus of epoxy resins. (—) 828-I, (---) 828-II, (· · ·) 828-III, (- · - ·) 834-I, (— — —) 834-II.

In a previous paper [4], when the variable tensile strength of the fibre was assumed, the mean axial compressive strength,  $(\bar{\sigma}_f)_c$ , of the fibre is given by

$$(\bar{\sigma}_f)_c = (\bar{\sigma}_{f,l})_t (\bar{l})_c / (l)_t \quad (4)$$

where  $(\bar{\sigma}_{f,l})_t$  is the mean tensile strength of the fibre at length  $L$  and is given by Equation 2,  $(\bar{l})_c$  is the mean fragment length in compression, and  $(\bar{l})_t$  is the mean fragment length in tension.

The relationship between both the mean fragment length  $(\bar{l})_t$  in tension and  $(\bar{l})_c$  in compression of composite systems including reinforcing fibres having tensile strength distributions and temperature are shown in Figs 4 and 5, respectively.

When all the fragments have been reduced to less than the critical fibre length, no further elongation of the specimen will cause the fibre to break. When the fibre finally breaks into many pieces, we have previously proposed that this considerable tensile strength is the tensile strength at the length just before the final-fragment lengths [14].

If  $\bar{l}$  represents the average value of the final fragment length,  $K\bar{l}$  the first embedded length, and  $k\bar{l}$  the length just before the length  $\bar{l}$ , then, the average value  $\bar{L}^x$  of the length just before the fragment length with  $\bar{l}$  is given by [9]

$$\bar{L}^x = \frac{4}{3}\bar{l} + \sum_{k=3}^{k-1} k\bar{l} \left( \frac{4}{k-1} \right) \left( \frac{1}{3} \right)^{k-1} + K\bar{l} \left( \frac{2}{K-1} \right) \left( \frac{1}{3} \right)^{K-2} \quad (5)$$

The average value  $\bar{L}^x$  of the length just before the length  $(\bar{l})_t$  from the mean fragment length  $(\bar{l})_t$  (Fig. 4) in tension according to Equation 5 can also be calculated. Furthermore, the mean tensile strength  $(\bar{\sigma}_{f,l})_t$  of the fibres is determined by substituting the value into Equation 2 using a method described in previous papers [4, 8].

Fig. 6 shows the relationship between the mean value of fibre axial compressive strength  $(\bar{\sigma}_f)_c$

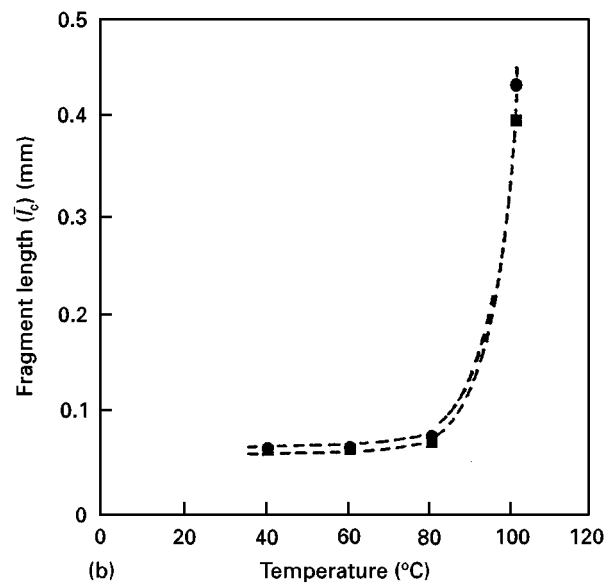
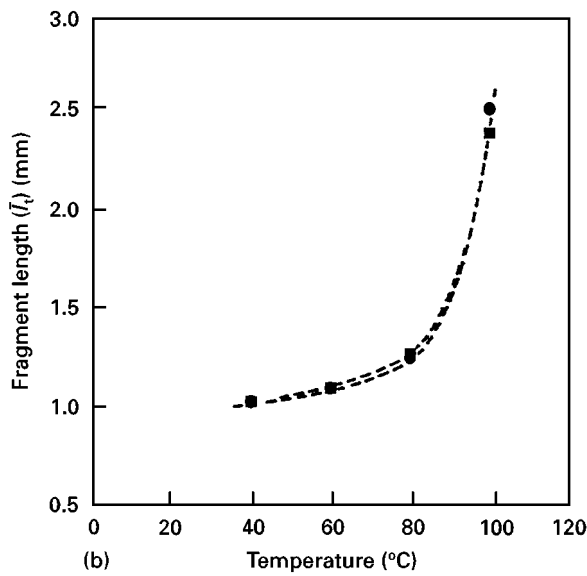
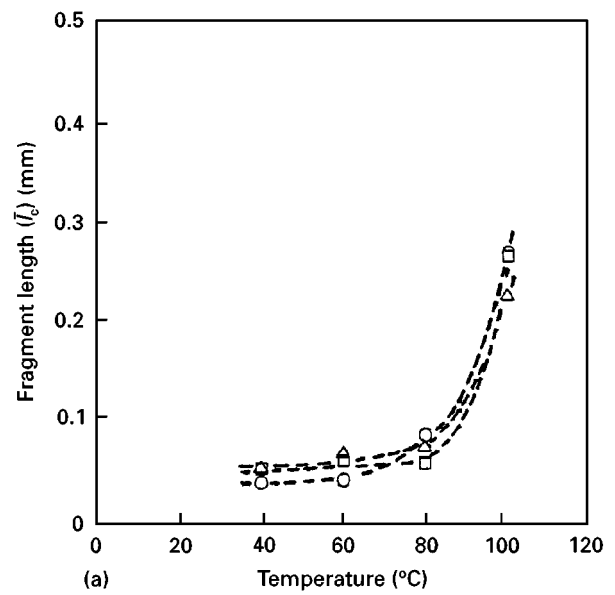
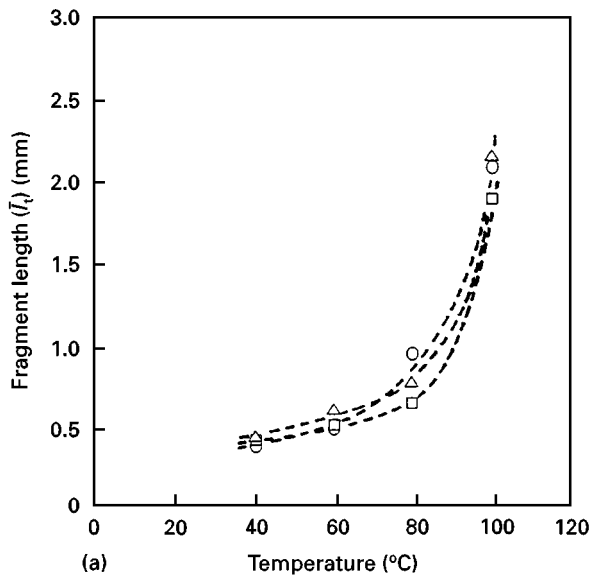


Figure 4 Relationship between temperature and mean fragment length in tension. (a) Epikote 828 system, (○) I, (□) II, (△) III; (b) Epikote 834 system, (●) I, (■) II.

Figure 5 Relationship between temperature and mean fragment length in compression. (a) Epikote 828 system, (○) I, (□) II, (△) III; (b) Epikote 834 system, (●) I, (■) II.

estimated from the mean fragment length ( $\bar{l}$ )<sub>t</sub> (Fig. 4) in tension, the mean fragment length ( $\bar{l}$ )<sub>c</sub> (Fig. 5) in compression, and the mean tensile strength ( $\bar{\sigma}_{t,i}$ ) of the fibre according to Equation 4, and temperature. With these systems, in the same manner as observed in the carbon and aramid fibres [1–7], the estimated compressive strength decreases with increasing temperature up to 80 °C. As indicated elsewhere [1–7], it is conceivable that the radial force compressing the fibre decreased by both the decrease in residual thermal stress and Young's modulus of the resin matrix with increasing temperature may cause a temperature dependence of the estimated value of the fibre axial compressive strength.

The estimated compressive strength increases greatly above 80 °C. It is conceivable that the fibre buckles, and conditions for application of the above-mentioned Equation 3 cannot be satisfied above 80 °C [1–7]. Accordingly, further details are discussed for results obtained at a temperature range lower than 80 °C.

When a fibre is embedded in the resin and the system is allowed to cure, the thermal stress ( $P$ )<sub>T</sub> working perpendicular to the fibre–resin interface is approximately given by [11]

$$(P)_T = \frac{(\alpha_m - \alpha_f) E_m \Delta T}{1 + \nu_m} \quad (6)$$

where  $\alpha$  is the thermal expansion coefficient,  $E$  is Young's modulus,  $\nu$  is Poisson's ratio,  $\Delta T$  is the difference in temperature from the moulding temperature, and the subscripts  $m$  and  $f$  denote matrix and fibre, respectively. The thermal expansion coefficient  $\alpha_m$ , Young's modulus  $E_m$ , and Poisson's ratio  $\nu_m$ , required to calculate thermal stress, were measured. The thermal stress ( $P$ )<sub>T</sub> was then calculated from Equation 6 as in a previous paper [6]. The thermal stress ( $P$ )<sub>t</sub> calculated from Equation 6 is shown in Fig. 7. We have utilized a thermal expansion coefficient,  $\alpha_f$ , perpendicular to the fibre axis, where  $\alpha_f$  is  $9.9 \times 10^{-6} \text{ } ^\circ\text{C}^{-1}$

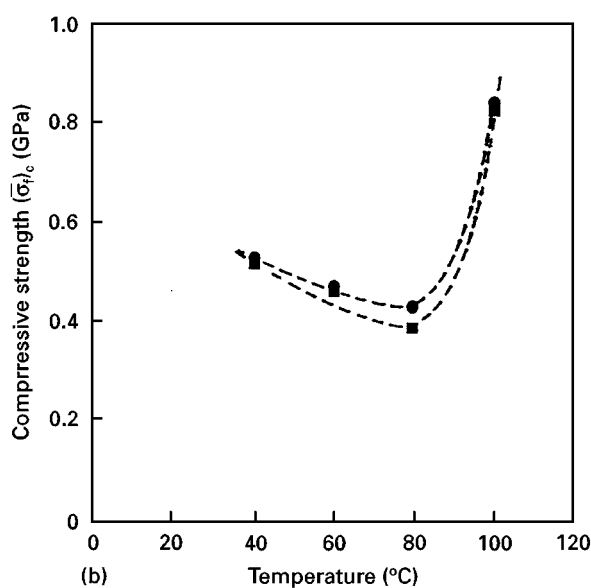
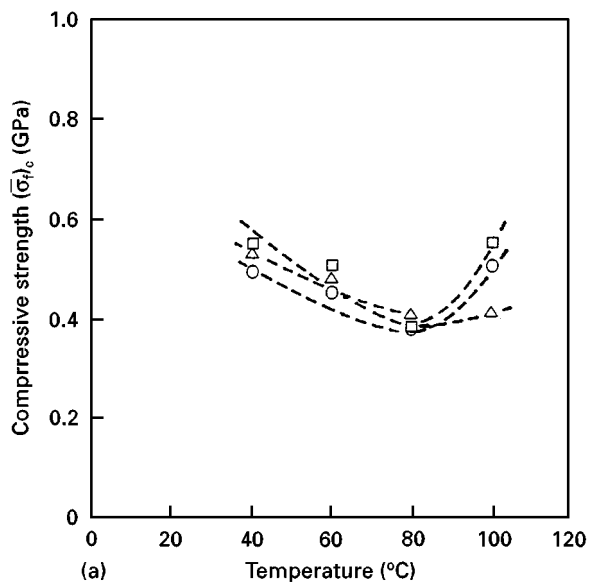


Figure 6 Relationship between temperature and estimated mean compressive strength of the fibre. (a) Epikote 828 system, (○) I, (□) II, (△) III; (b) Epikote 834 system, (●) I, (■) II.

[12] for graphitized fibre. In addition, we have assumed that this value is constant in the temperature range of this experiment.

Fig. 8 shows the relationship between the estimated mean compressive strength ( $\bar{\sigma}_r$ )<sub>c</sub> (Fig. 6) and the thermal stress ( $P$ )<sub>T</sub> (Fig. 7) obtained through the function of temperature. With these systems, the estimated mean compressive strength of graphitized fibre decreases linearly with decreasing thermal stress.

As indicated in previous papers [1–7], it is conceivable that the real compressive strength of fibres is the strength when the radial compressive force, i.e. the residual thermal stress in this experiment, is zero. Accordingly, we have considered the value obtained by extrapolating the straight line in Fig. 8 to ( $P$ )<sub>T</sub> = 0 as the real compressive strength of graphitized fibre. These real values of fibre for various epoxy resins are shown in Fig. 9. Regardless of Young's modulus of the epoxy resin matrices, the estimated axial compressive

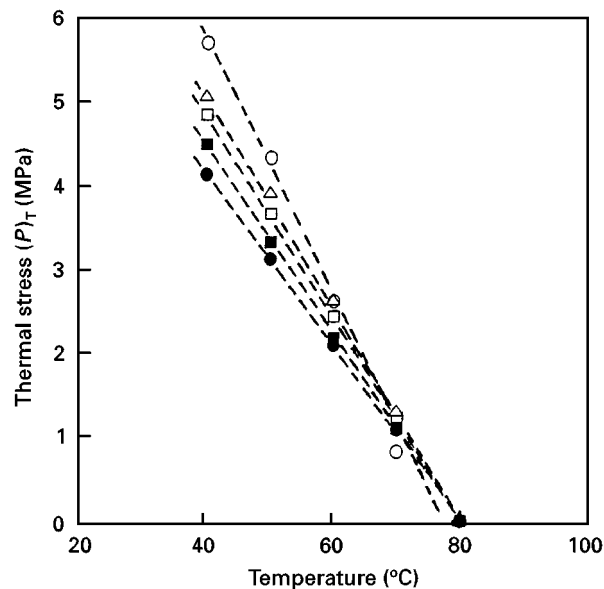


Figure 7 Relationship between thermal stress and temperature. (○) 828-I, (□) 828-II, (△) 828-III, (●) 834-I, (■) 834-II.

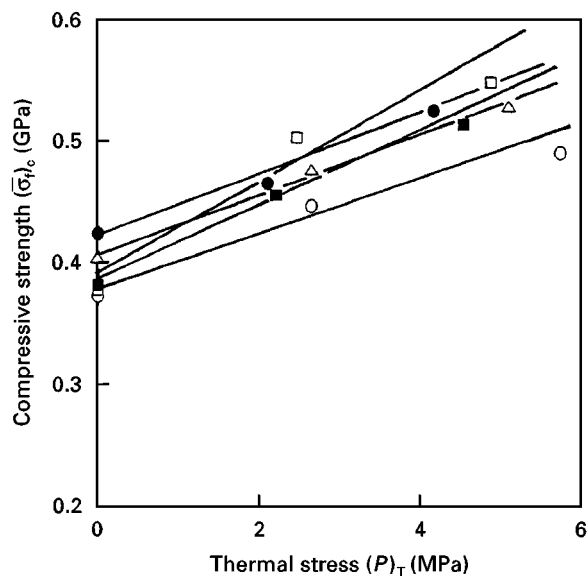


Figure 8 Relationship between thermal stress and estimated mean compressive strength of the fibre. (○) 828-I, (□) 828-II, (△) 828-III, (●) 834-I, (■) 834-II.

strengths obtained by extrapolating, are almost the same:  $\sim 0.4$  GPa. Thus the compressive strength estimated in this manner is the real compressive strength used in this experiment. Furthermore, this value (0.4 GPa) is almost the same as that obtained earlier [7].

Fig. 10 shows the relationship between the Young's modulus,  $E_m$ , of epoxy resin matrices (Fig. 3) and the estimated compressive strength (Fig. 6) obtained through the function of temperature. The compressive strength increases with increasing Young's modulus of the epoxy resin. It is conceivable that the radial force compressing the fibre increases with increasing Young's modulus. Consequently, when the fibre is embedded in the resin matrix with higher modulus, it can be confirmed that a higher compressive strength of the fibre is realized.

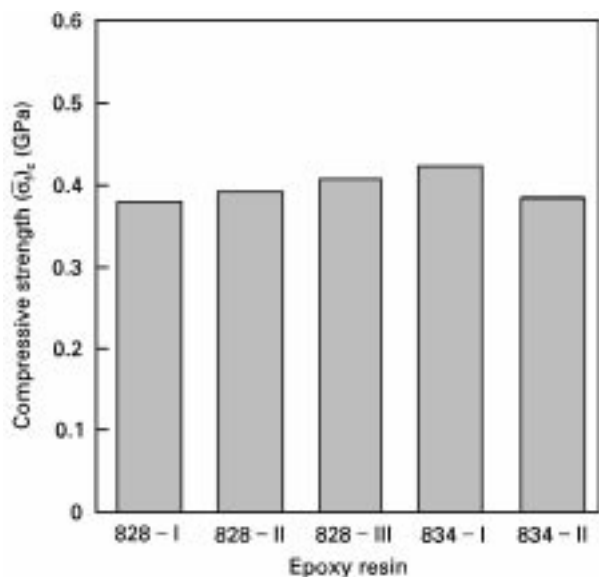


Figure 9 Compressive strength of the fibre for various epoxy resin systems.

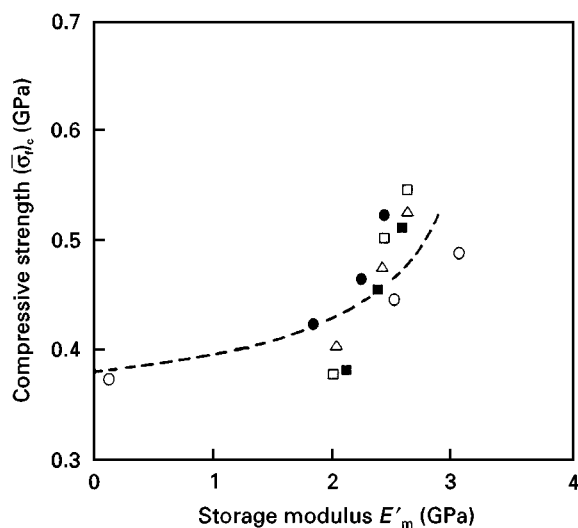


Figure 10 Relationship between Young's modulus of the epoxy resins and the estimated mean compressive strength of the fibre. (○) 828-I, (□) 828-II, (△) 828-III, (●) 834-I, (■) 834-II.

#### 4. Conclusion

By measuring the lengths of the broken pieces of the fibre embedded in the resin matrix and estimating the mean tensile strength from the length just before the final fragment length in tension, attempts have been made to estimate the fibre axial compressive

strength of pitch-based graphitized fibre, and the effects of Young's modulus of the epoxy resin on the compressive strength was investigated.

The estimated compressive strength of fibres decreases with increasing temperature. This decrease in compressive strength may be accounted for by a decrease in the radial compressing force due to a decrease in the residual thermal stress.

There is a linear relationship between the estimated compressive strength and radial compressive force in the temperature range from room temperature to 80 °C. The estimated compressive strength of the fibre increases with increasing Young's modulus of the epoxy resin. In order to obtain reinforcing fibres with a higher compressive strength, it will be necessary to use a resin matrix with higher modulus.

By taking into consideration previous results [1-7], it was found that a fibre with higher compressive strength can be developed by increasing the degree of orientation or face spacing of the crystal, by decreasing the crystal size, by decreasing the fibre diameter, by surface- and size-treatments, and by increasing Young's modulus of the matrix.

#### References

1. M. MIWA, T. OHSAWA, M. KAWADE and E. TSUSHIMA, *Reinf. Plastics Jpn* **35** (1989) 199.
2. T. OHSAWA, M. MIWA, M. KAWADE and E. TSUSHIMA, *J. Appl. Polym. Sci.* **39** (1990) 1733.
3. M. MIWA, A. TAKENO and Y. LIU, *Reinf. Plastics Jpn* **37** (1991) 289.
4. M. MIWA, E. TSUSHIMA and J. TAKAYASU, *J. Appl. Polym. Sci.* **43** (1991) 1467.
5. M. MIWA, A. TAKENO, Y. LIU, A. WATANABE, J. TAKAYASU and E. TSUSHIMA, *Reinf. Plastics Jpn* **38** (1992) 433.
6. M. MIWA, Y. LIU, H. TSUZUKI, A. TAKENO and A. WATANABE, *J. Mater. Sci.* **31** (1996) 499.
7. M. MIWA, A. TAKENO, Y. MORI, T. YOKOI and A. WATANABE, *ibid.* **31** (1996) 2957.
8. M. MIWA, T. OHSAWA and K. TAHARA, *J. Appl. Polym. Sci.* **35** (1978) T-19.
9. M. MIWA, T. OHSAWA and A. TOMITA, *Koubunshi Ronbunshu* **41** (1984) 353.
10. L. E. NIELSEN, "Mechanical Properties of Polymer and Composites", Marcel Dekker, New York (1974) p. 177.
11. G. GERARD and A. C. GILLBERT, *J. Appl. Mech. (ASTM)* **24** (1957) 355.
12. A. KOBAYASHI, in "20th Air Plane Symposium", Japan (1982) p. 70.

Received 30 June 1997

and accepted 22 April 1998